Chemical routes to materials

The role played by different active hydrogen sources in the microencapsulation of a commercial oligomeric diisocyanate

Mónica V. Loureiro[1] , Mahboobeh Attaei[2] , Sofia Rocha[1] , Mário Vale[1] ,
João C. Bordado[1] , Ricardo Simões[3] , Isabel Pinho[4] , and Ana C. Marques[1,*]

[1] *CERENA, Departamento de Engenharia Química, Instituto Superior Técnico, Universidade de Lisboa, Avenida Rovisco Pais, 1049-001 Lisbon, Portugal*

[2] *CQE, Departamento de Engenharia Química, Instituto Superior Técnico, Universidade de Lisboa, Avenida Rovisco Pais, 1049-001 Lisbon, Portugal*

[3] *Instituto Politécnico do Cávado e do Ave – IPCA, Campus do IPCA, Barcelos, Portugal*

[4] *CIPADE-Indústria e Investigação de Produtos Adesivos, SA. Av. Primeiro de Maio 121, São João da Madeira, Portugal*

ABSTRACT

The present paper regards the development of polyurea/polyurethane (PUa/PU) and PUa/PU–silica hybrid shell microcapsules (MCs), loaded with Ongronat®2500, a commercial type of oligomeric methylene diphenyl diisocyanate with increased functionality, as core material. Ongronat® 2500 has a wide range of applications either for the production of rigid polyurethane foams and as cross-linking or self-healing agent. The MCs were achieved by a facile, one-pot process, consisting of an oil-in-water microemulsion system combined with interfacial polymerization processing, employing a higher reactivity isocyanate, toluene diisocyanate, to competitively contribute to the shell formation. Ethylenediamine, polyethylenimine (PEI), triethoxy(octyl)silane (n-OTES) and 3-(2-aminoethylamino) propyltrimethoxysilane (aminosilane) were tested as active, or "latent" active hydrogen (H) sources, and their effect on the MCs morphology, encapsulation yield, shelf life, shell's chemical structure and thermal stability was assessed. The MCs are aimed at the development of a new generation of adhesive formulations, which are mono-component, self-reactive, eco-friendly and with low health hazards, for industries such as the footwear, construction, aerospace and automotive. MCs' characterization was performed using Fourier transformed infrared spectroscopy, thermogravimetric analysis and scanning electron microscopy. It was possible to obtain MCs with a high loading of Ongronat®2500, exhibiting a core–shell morphology, an increased shell resistance to temperature and improved shelf life. The combination of PEI and n-OTES led to the best compromise between encapsulation yield and shelf

---

Address correspondence to E-mail: ana.marques@tecnico.ulisboa.pt

Ⓐ Springer

life. Finally, a confinement effect of the encapsulated macromolecules is herein shown for the first time, by the drastic narrowing of the NCO peak at the FTIR spectrum of the MCs.

Introduction

High quality, strong and long-lasting adhesives used in the footwear, construction, automotive and aerospace industries typically include highly reactive isocyanate species in their formulation, in order to provide the required high strength adhesive joints. These are bicomponent adhesives, supplied in two components to be posteriorly mixed, one being based on isocyanate species, to act as cross-linkers and the other being a polyol base (OH prepolymer). The high reactivity of isocyanates, their solubility in various solvents, the easiness of wetting and the capability to penetrate material porous structures, with the formation of covalent bonds and therefore strong mechanical interlocks, make these chemicals appealing in applications such as the adhesives industry, but also for self-healing purposes [1, 2].

The ongoing need for improving the ingredients compatibility while minimizing the hazards associated with the various components, as well as product degradation, is the driving force for the exploration of microencapsulation in the adhesives field. Indeed, microencapsulation promotes reduced risks related to the handling and storage of hazardous ingredients included in adhesive formulations, as well as tuned control of the rate and moment at which the encapsulated compound is released, being nowadays applied in a large range of applications [3–6]. In the present work, encapsulation of isocyanate species is pursued to enable the development of a new generation of self-reactive, mono-component adhesives (1 K), with reduced health hazards during handling, absence of manufacturing (weighing) errors and less packaging derived waste. Aligned with the constant demand of legislation and an increasing need for environmental awareness and worker protection, these mono-component adhesive formulations represent a great step forward in innovation and sustainability.

Isocyanate's microencapsulation is typically achieved by an oil-in-water (O/W) microemulsion system combined with interfacial polymerization, which involves the addition of, at least, two reactants in a pair of immiscible liquids. One of the liquids is preferably an aqueous solution, forming the continuous phase (W phase) and the other, the dispersed phase, is composed of the isocyanate to encapsulate (O phase). To disperse two immiscible phases, high shear rate mixing and a third material, emulsifier/surfactant, are employed. This is followed by diffusion of the reactants, which become in contact at the interface of the oil droplets of the emulsion system. Both phases (water-based and oil-based solution) contain reactive species (OH groups and NCO groups, respectively) which react together to form an initial thin polyurea (PUa) or polyurethane (PU) polymeric shell. It should be noted that the initial reaction of water and isocyanate forms an unstable carbamic acid intermediate that immediately decomposes to amine and CO_2 [7]. Further reaction with isocyanate results in PUa. The thickness of the shell increases until the point when no more reactant species are allowed to be in contact [1, 2]. The polymerization is controlled mostly by diffusion, so the growth's rate of the microcapsules (MCs)' shell will decrease as the shell thickness increases [8].

An adequate choice of the oil and water phase composition must be done, since the affinity of the constituents of these two phases will determine the resulting MCs' structure. Also, synthesis parameters, such as the synthesis temperature, concentration of the employed materials, reaction time, emulsification time and speed, as well as stirring conditions will affect the quality of the synthesized MCs [8]. The aromatic or aliphatic structures, as well as branched or linear structures of the isocyanates and active H sources greatly influence the MCs morphology, porosity, permeability and thermal and mechanical resistance, resulting thus on an impact on the release performances, or shelf life of the MCs [8]. The formation of a 3D cross-linked polymer network and the presence of aromatic structures typically result in more stable MCs with higher thermal and mechanical resistance.

The encapsulation of oligomeric or prepolymeric isocyanates by a PU/PUa shell is potentially

preferred, since it brings higher reactivity in what regards the formation of a 3D polymeric structure in adhesive joints or self-healing applications. However, the encapsulation of these species, including the commercially available ones, is scarcely found in the literature and, according to our experience, it frequently involves synthesis issues due to high viscosities and difficulty to control the high reactivities, unless an organic solvent is added to the isocyanate solution [9, 10].

The major efforts, reported in the literature, regarding the microencapsulation of isocyanate compounds in the liquid state date from 2008, with the encapsulation of monomeric isophorone diisocyanate (IPDI). Yang et al. [11] have reported for the first time, the successful microencapsulation of monomeric IPDI, to be employed as a healing agent, via interfacial polymerization, resourcing to a 2,4-TDI prepolymer, as a higher reactivity isocyanate compound for the shell formation. They reported the addition of 1,4-butanediol to the W phase as active H source and chain extender. A similar methodology was followed by Sondari et al. [12] who reported in 2010 the successful encapsulation of the same monomer using glycerol as active H source and chain extender. Di Credico et al. [13] reported the encapsulation of IPDI, by PU and double-layered PU/poly(urea-formaldehyde) PU/PUF shells, obtaining core fractions of 49 wt% and 68 wt% for PU and PU/PUF MCs, respectively. Still regarding the encapsulation of IPDI, Kardar [14] reported a synthesis where 1,4-butanediol, 1,6-hexanediol and glycerol were used for achieving a higher encapsulation yield. Ming et al. [15] prepared MCs of IPDI core and PUa/melamine formaldehyde double-layered shell, using Desmodur L-75 as the PU part of the shell forming material. In this case, the use of polyetheramine and a prepolymer of melamine formaldehyde led to a core (IPDI plus ethyl acetate) fraction of 78% [15]. Finally, in a previous work from the team and still in what regards IPDI encapsulation, Attaei et al. reported in 2018 the preparation of PUa/PU shell MCs containing high loadings of IPDI in the core to enable the production of mono-component, eco-friendly and safer adhesive formulations for the footwear industry [3]. In that case, Ongronat®2500, with higher reactivity than IPDI, was employed as shell forming material. Four different active H sources were tested, 3-(2-aminoethylamino) propyltrimethoxysilane, tetraethyl orthosilicate, diethylenetriamine (DETA) and

3-isocyanatopropyltriethoxysilane (IPES) aiming at achieving a high encapsulation yield. The incorporation of the multifunctional isocyanate silane in the O phase, as "latent" active H source, led to the formation of impermeable PUa/PU–silica hybrid shell MCs with more than 60 wt% of pure encapsulated IPDI. Silanes can be considered "latent" active H sources, since when added to the synthesis, they are not readily able to react with the isocyanate NCO groups. In the presence of water, their alkoxy groups suffer hydrolysis, with formation of silanol Si-OH groups, which will react with NCO, forming urethane moieties. Adhesive joints prepared with encapsulated IPDI were found to exhibit the same peeling strength as the ones with non-encapsulated IPDI, which reveals the effective release and cross-linking ability of the encapsulated IPDI [3]. Other monomeric isocyanates, such as hexamethylene diisocyanate (HDI), have also been encapsulated, namely in the works reported by Huang et al. and Wu et al., where MDI prepolymers were employed as shell forming material and the work of Nguyen et al. where a commercial MDI and HDI trimer, Suprasec® 2020, was used [16–18]. In these works, active H sources, such as 1,4-butanediol, polyethylene imine (PEI), pre-hydrolyzed TEOS and triaminopyrimidine tri-amine, were employed. Moreover, hexamethyldisilazane, alkylamine, fluorinated aromatic amine and perfluoride amine compounds were also used as hydrophobic agents to increase the core content and shelf life of the MCs [18].

Ma et al. [10] reported the preparation of MCs containing encapsulated polyaryl polymethylene isocyanates (PAPI), to which 1,4-butanediol, ethylene glycol and 1,2-diaminoethane were employed as active H sources during the synthesis. NCO content in the core was quantified at 23 wt% by titration analysis, and it was found to drop in a period of 30 days from 23 to 6%, when the MCs were in contact with the moisture of the atmosphere. Haghayegh et al. published a work in 2016, where the goal was to develop self-healing agents based on isocyanate functionality [9]. Faster curing rate and more appropriate physical properties were expected for moisture curing of bulky isocyanate molecules than the low molecular weight monomeric analogous. In this sense, they developed the encapsulation of an IPDI prepolymer with 15.7 wt% NCO, employing a TDI prepolymer as shell forming material, also prepared in the laboratory, with 19.2 wt% NCO. Both of these

prepolymers were diluted with 60 wt% of chlorobenzene (b.p. of 132 °C) and, therefore, the final encapsulation yield will account not only for the isocyanate species, but also for the organic solvent.

The previously referred works clearly evidence the contribution of the active H source type on the MCs' morphology and isocyanate encapsulation yield. The NCO groups react with the OH or NH groups from the active H sources to form urea or urethane moieties, with the main factor that influences the activity and reaction of these chemicals in emulsions being their solubility and diffusion rate towards the water–oil interface. The higher the partition coefficient parameter, the higher the reactivity of the active H sources and the extent of the reaction and, therefore, the thicker the shell [14]. Moreover, different chemical structures of the same category of active H sources also influence the shell morphology, in the sense that higher functionality (more OH or NH groups density) results in more readily available sites for reaction, leading to a high degree of cross-linking and, therefore, an increased hardness of the shell. Also, linear structure active H sources lead to a lower mechanical resistance shell, which might result in the wrinkling of the same. Wrinkling on the surface of the shell might be also derived from fast reactions between the active H sources and NCO [10]. On the other hand, branched active H sources lead to a thicker shell formation due to the presence of bulkier groups [10, 14, 16, 19]. Therefore, a strategic selection of the active H sources employed in the MCs' synthesis must have into account the required specifications for the MCs.

The present paper regards the microencapsulation of a commercial, readily available type of oligomeric MDI, Ongronat® 2500, with an increased functionality of 31 wt% NCO, to be used as a cross-linker in polyurethane (PU) adhesive formulations, or as self-healing agent in smart applications. It is also quite used for the production of rigid PU foams for the construction industry. To the best of our knowledge, this has never been reported before. Ongronat® 2500 is a solvent-free, medium viscosity liquid at room temperature and is composed of monomers, dimers and trimers of MDI, which makes it an oligomeric compound.

The novelty of this work relies on (1) the microencapsulation of Ongronat® 2500, at a high loading, by a PU/PUa and PU/PUa–silica hybrid shell, using a minor content of organic solvent, 25 wt% versus the 60 wt% found in the literature [9]; (2) the use of a monomeric higher reactivity diisocyanate TDI (2,4 isomer) as shell forming agent. Its low viscosity contributes to the employment of the lower amount of solvent just described; (3) the evidence of a confinement effect of the encapsulated macromolecules revealed in the FTIR spectra; (4) optimization studies involving multifunctional active H sources aiming at a faster formation of the MCs' shell and a higher encapsulation efficiency, such as poly(ethyleneimine), which greatly contributes to the 3D cross-linked polymer network of the shell; (5) the addition of 3-(2-aminoethylamino) propyltrimethoxysilane (aminosilane) and triethoxy(octyl)silane (n-OTES), which according to our knowledge have not yet been reported in the literature for this application. They not only contribute as "latent" active H source, as their previous hydrolysis is necessary in order to form silanol groups which will further be able to react with the isocyanate NCO groups, but also result on an enhanced PUa/PU–silica hybrid shell. The amino groups of the silane will react with NCO groups leading to the formation of urea moieties within the shell, while the long aliphatic carbohydrate chain, namely the 8 carbons tail of n-OTES is anticipated to contribute to the hydrophobicity required for longer shelf-life MCs, which might prevent moisture from penetrating across the shell. Moreover, the siloxane moieties, responsible for the hybrid character of the shell's material, are known to promote an improved mechanical strength and thermal resistance of the MCs.

Materials and method

Materials

The commercial MDI oligomer, Ongronat® 2500, the compound to be encapsulated, was kindly supplied by BorsodChem. The shell forming agent isocyanate, TDI (2,4 isomer), was obtained from Dow Chemicals. Regarding the active H source compounds, the aminosilane 3-(2-aminoethylamino) propyltrimethoxysilane (A) (with 90% purity) was purchased from VWR Chemicals, triethoxy(octyl)silane (n-OTES) and poly(ethyleneimine) (PEI) aqueous solution ($\overline{M_w}$ 60000, 50 wt% in H$_2$O) were supplied from Sigma-Aldrich and ethylenediamine (EDA) was supplied from Fluka. The emulsifier Gum Arabic

(GA) was obtained from LabChem, and the solvent n-hexane (with 95% purity) was purchased from VWR Chemicals. All chemicals were used as received, without further purification.

Method

In situ encapsulation of isocyanate

MCs were prepared via an oil-in-water (O/W) microemulsion system combined with in situ polymerization at the O/W interface. The O/W microemulsion was prepared through vigorous stirring of a mixture of the immiscible water and oil phases, at 3400 rpm with an Ultra-Turrax (IKA T25 digital ULTRA TURRAX, Germany), during 10 min at room temperature (RT), in order to obtain a stable emulsion.

The synthesis procedure and the respective parameters employed in this work are an adaptation from the process developed by our team, described in Attaei et al. [3]. Table 1 summarizes the primary materials used and the main parameters involved. The W and O phases were left constant for all runs. The W phase was made up of 4.7 wt% GA in water, while the O phase consists of TDI (19 wt% of the O phase), Ongronat® 2500 (56 wt% of the O phase) and an inert organic solvent of low boiling point, n-hexane (25 wt% of the O phase). After 30 min of mechanical stirring at 400 rpm, with a mechanical stirrer, Heidolph RZR 2051 control, the active H sources were added dropwise to the emulsion system, except for Ref_MCs to which no active H source was added. Synthesis temperature was set at 65 °C. The type and amount of active H source added per synthesis are listed in Table 1, as well. The Ref_MCs

synthesis followed the same procedure as the remaining MCs, except that no active H source was added.

It is important to state that the present work aims to study the effect of different active H sources in the MCs properties, for the precisely same synthesis conditions, and so no optimizations were conducted for each case.

During the mechanical stirring phase, samples were withdrawn and checked under the optical microscope. This provides crucial information regarding the shell formation and maturation and, hence, synthesis completion. The reaction was maintained at 65 °C and stirring rate 400 rpm until the MCs' shell attained enough maturity (stiffness) to tolerate the pressure applied during the filtration procedure. The MCs were then filtrated using a vacuum filtration system, while extensively washed with Milli-Q water, to avoid particle aggregation. The MCs were dried at RT for 24 h and a free-flowing powder was obtained.

Characterization

The adopted techniques for the MCs' characterization include: optical microscopy, scanning electron microscopy (SEM), Fourier transformed infrared spectroscopy (FTIR) with attenuated total reflectance (ATR) accessory, thermogravimetric analysis (TGA) and first derivative curves (DTG).

Optical microscopy

A Kruss, MSZ 5600 optical microscope was used in order to evaluate the stability of the emulsion,

Table 1 MCs' synthesis parameters: water and oil phase and active H source employed. Average maximum temperature achieved during the synthesis is 65 °C

MCs' acronym[a]	Water phase	Oil phase	Active H source (wt% of total emulsion)
Ref_MCs	Water + GA	Ongronat®2500 + TDI + n-hexane	–
PEI_MCs			aq. PEI solution at 10 wt% (1.9 wt%)
EDA_MCs			Water (3.7 wt%) + EDA (3.7 wt%)
A_MCs			Aminosilane (5.4 wt%)
n-OTES_MCs			n-OTES (4.9 wt%)
n-OTES_PEI_MCs			n-OTES (4.7 wt%) + aq. PEI solution at 10 wt% (4.7 wt%)

[a]The letters preceding "MCs" refer to the active H source employed in the synthesis of the MCs

droplets' size and the MCs' shell maturity during the synthesis procedure (Fig. 1).

Scanning electron microscopy (SEM)

The morphology, size distribution and average shell thickness of the obtained MCs were assessed through SEM, with a field emission gun scanning electron microscope FEG-SEM operating at 15 kV, JEOL JSM7001F (JEOL, Tokyo, Japan). The samples were previously coated with a conductive Au/Pd thin film, through sputtering, using a Quorum Technologies sputter coater, model Q150T ES. The shell thickness and size distribution of the MCs were evaluated using photomicrographs obtained through SEM, employing the Fiji software, in samples of 70 MCs.

Fourier transformed infrared spectroscopy (FTIR)

The relative isocyanate encapsulation efficiency, as well as the chemical structure of the MCs' shell, was assessed by FTIR spectroscopy with the ATR accessory. Spectra of the isocyanate compounds and active H sources employed in the syntheses, as well as those of the MCs, were obtained for such purpose. The FTIR equipment used was a Spectrum Two from PerkinElmer, equipped with a Pike Technologies MIRacle® ATR accessory. The spectra were obtained using 8 cm^{-1} resolution and a data collection of 8 scans.

Thermogravimetric analysis (TGA)

TGA was performed, using a HITACHI STA 7200 Thermal Analysis System equipment, under a controlled nitrogen atmosphere with a flow of 200 ml/ min, at a temperature increase rate of 10 °C min^{-1}, in the range of 30–600 °C. The analysis of the resulting thermograms, as well as of the obtained derivative curves (DTG), enabled to draw conclusions regarding to which isocyanate source was involved in the shell formation and which one was effectively encapsulated. This technique was also used to corroborate FTIR analysis results.

Results and discussion

Figure 1 gives an insight on the morphology evolution during the synthesis, in the case of the A_MCs, until the free-flowing powder consisting of the MCs (Fig. 1c) is obtained. Figure 1a shows the microemulsion just before addition of the active H source (aminosilane), while Fig. 1b shows the starting of the solid shell formation, after addition of the active H source.

The morphology and size distribution of the MCs were assessed by SEM. The photomicrographs of the obtained MCs are displayed in Fig. 2 where a general view of each sample, at low magnification, is displayed. As it is possible to observe, all the syntheses led to loose, disaggregated MCs, with a fairly spherical shape and a rough surface. The shell roughness might be caused by fluid-induced shear forces, due to the mechanical stirring during the synthesis, as well as inhomogeneous reaction kinetics and/or fast reaction between the isocyanate, the added active H sources and water [11, 14, 16, 20]. The MCs that show a more wrinkled surface are the Ref_MCs and the EDA_MCs. The Ref_MCs did not have the extra contribution of active H sources to the shell formation, which led to a thinner and less resistant shell, while the EDA_MCs were the ones to which a small size linear active H source was added,
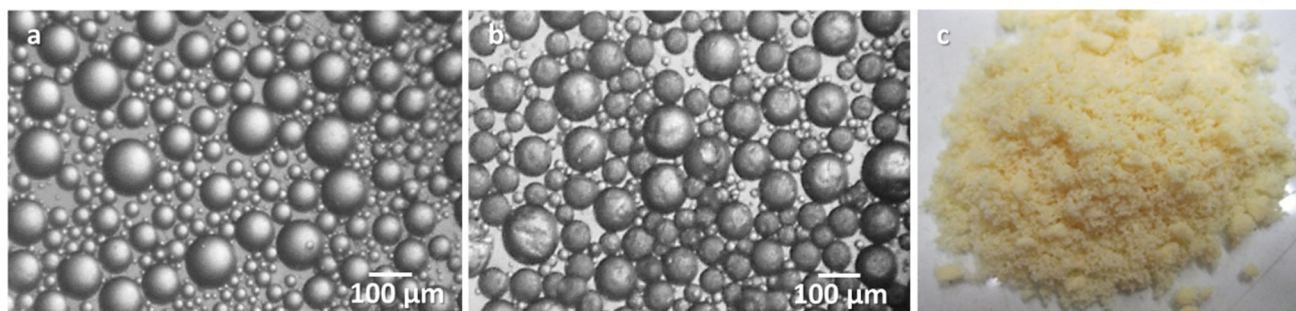
Figure 1 MCs morphology evolution during synthesis: **a** microemulsion before addition of the active H source, **b** shell formation after addition of the active H source, **c** free-flowing powder consisting of the MCs after synthesis (scale 1:1).
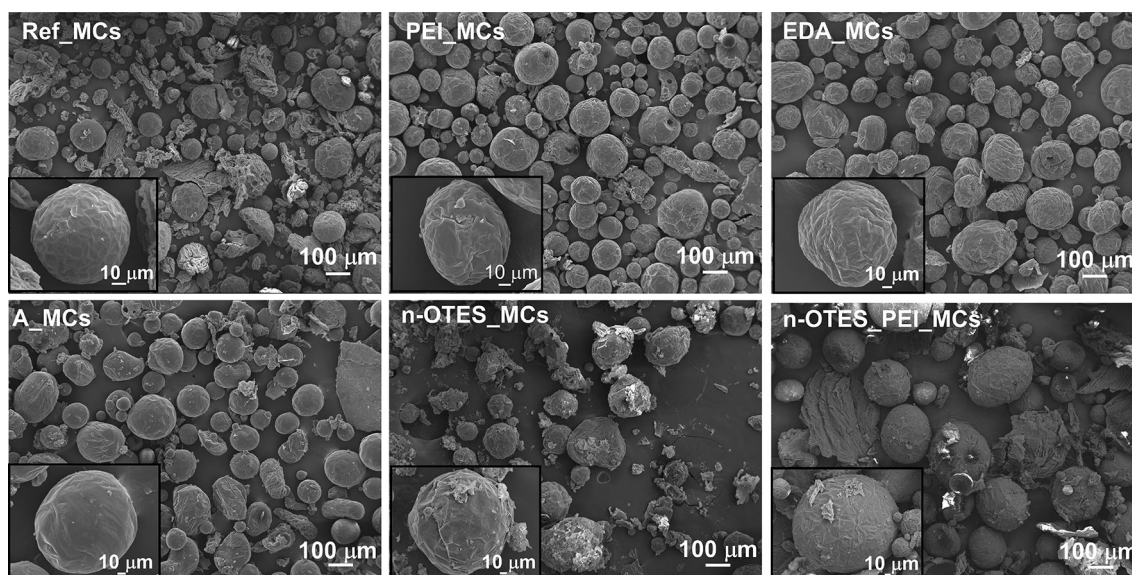
Figure 2 SEM photomicrographs of the obtained MCs using 80X amplification, scale bar = 100 μm. The inset shows an amplified single MC for each synthesis to better observe the surface morphology.

also leading to a lower mechanical resistance when comparing to the MCs to which branched active H sources were added during the synthesis.

Since all syntheses were carried out under the same emulsification and mechanical stirring velocities, temperature range, organic and aqueous mixture, it is reasonable to assume that the observed morphological and encapsulation yield changes are due to the different active H sources employed.

It is possible to conclude that, for the applied synthesis conditions, the MCs to which only NH (amine) based active H sources were added during the synthesis, seem to have a more round and homogeneous shape and less debris, when comparing with the Ref_MCs, n-OTES_MCs and n-OTES_PEI_MCs (Fig. 2). The debris might be originated from MCs that were broken during the synthesis due to the mechanical stirring, as well as from some polymerization side-reactions that might have occurred in the reaction medium, possibly due to a non-perfectly stable microemulsion. These latter MCs show that more optimization trials would be required. However, since the aim of the present work was to study the effect of different active H sources for the same synthesis conditions, these samples were also involved in the remaining characterization procedures, in order to conclude about their encapsulation efficiency and shelf life.

The MCs were deliberately crushed in order to identify their morphology. Observing the photomicrographs present in Fig. 3, it is possible to conclude that all syntheses led to core–shell MCs. The shell thickness values are displayed in Table 2. For the shell thickness and mean deviation calculation, several measurements were performed at the cross sections. Also, the MCs' diameter distribution has been analysed by the Fiji software (Supplementary File, S1) and their predominant diameter value is listed in Table 2. The ratio between the average shell thickness and the MC's diameter (S/D ratio) is also shown, with the higher values indicating a higher shell contribution to the MCs morphology.

The mechanical properties of the MCs are important for their final application as cross-linking agents for one component adhesives formulations, or as self-healing materials, with the requirements to be sufficiently robust to survive the blending within the formulation and adhesive joint preparation, or the structural material manufacture. However, they must be able to burst once in the adhesive joint by the effect of pressure, or after a damage event.

The Ref_MCs are the ones that exhibit a thinner shell, around 2 μm in thickness, and the lowest S/D ratio of 0.037, which might lead to unintended MCs breakage, which is in agreement with the photomicrographs observed in Fig. 2, where they are also the ones showing a higher amount of debris as well as a more wrinkled shell. Indeed, the active H sources led to changes in MCs' morphology, contributing to obtain a thicker shell. The shell formation process,
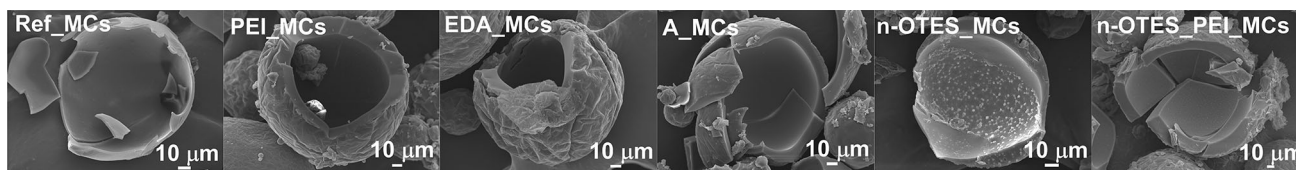
Figure 3 SEM photomicrographs of isolated MCs' cross sections from each synthesis, which were deliberately crushed. Scale bar = 10 μm.

Table 2 MCs' average shell thickness (S) and respective mean deviation, as well as MCs' diameter (D) and S/D ratio

MCs' acronym	S, Average shell thickness (μm)	D, MC's diameter (peak maximum, mode) (μm)	S/D (ratio)
Ref_MCs	2.19 ± 0.61	58[a]	0.037
PEI_MCs	18.36 ± 0.32	67[a]	0.27
EDA_MCs	14.31 ± 1.44	98[a]	0.15
A_MCs	12.17 ± 0.97	88[a]	0.14
n-OTES_MCs	9.81 ± 2.27	84 and 150[b]	0.12 and 0.065
n-OTES_PEI_MCs	15.86 ± 2.09	75 and 146[b]	0.21 and 0.11

[a]Monomodal lognormal distribution

[b]Bimodal Kernel smooth distribution

when PEI is added, is dominated by a cross-linking effect that comes from the branched structure rich in NH groups, of this amine-based polymeric structure, which is responsible by the thicker shells exhibited by PEI_MCs. Also, the original shell formed from the bulky macromolecule PEI active H source, is still somewhat rich in NH groups, which results in an ingrowth of the shell during some time after the synthesis end, which results in the higher S/D ratio value. Improved mechanical features of these MCs are expected. The addition of EDA, on the other hand, leads to the fast formation of the shell due to its fast diffusion through the shell towards the organic phase. The fast diffusion of EDA, the high reactivity of the primary aliphatic amines with NCO groups (relative uncatalyzed reaction rate at 25 °C is 1000 times higher than for primary hydroxyls and water with NCO [21]) resulting in inhomogeneous reaction kinetics, as well as its linear structure, which does not have the same contribution as a branched one to the MCs resistance, can also be accountable for the increase in the EDA_MCs' shell roughness [18, 22]. When the "latent" H sources, i.e. silanes (aminosilane and n-OTES), are added to the aqueous phase of the emulsions they are not readily able to react with the isocyanate NCO groups, being expected to hydrolyze, leading to the formation of silanol groups, which will then tend to react with NCO groups

forming urethane moieties, but also among them, forming siloxane moieties by condensation reactions [3].

Moreover, the amino groups from aminosilane (in A_MCs) tend to react with NCO groups forming PUa at the interface of the aqueous/organic phases, competitively with the reaction of NCO with water, due to a highly relative reaction rate. The two syntheses to which n-OTES was added as active H source are the ones with a higher mean deviation value in their shell thickness, which indicates a less homogeneous shell. The presence of n-OTES as "latent" active H source was also found to lead to a bimodal and more heterogeneous MC's size distribution, while the MCs with less heterogeneous size distribution are the Ref_MCs. The 8 C aliphatic chain, of hydrophobic nature, present in n-OTES molecule has low affinity with the aqueous phase and might contribute to local inhomogeneous compositions and reaction kinetics, together with different diffusion rate of the active H sources, water and the isocyanates present in the oil phase [11, 14]. The presence of n-OTES might also result in a less stable emulsion. n-OTES_PEI_MCs (PEI and n-OTES added) size distribution and shell thickness increase can be due to the conjuring of facts present for the synthesis of n-OTES_MCs and PEI_MCs. Indeed, it is possible to observe a significant increase in the S/D ratio for the

n-OTES_PEI_MCs, in comparison with the n-OTES_MCs. The addition of PEI to the synthesis leads to a higher degree of cross-linking in the shell, while n-OTES promotes the formation of PU/PUa–silica hybrid shell.

When comparing with the S/D ratio reported by Yang et al. in 2008, which are between 0.04 and 0.05, for isocyanate containing MCs with a PU shell, to which no active H sources were added, it is possible to conclude that its values resemble the ones obtained for the Ref_MCs [11]. Indeed, the active H source seems to play a crucial role in the strengthening of the MCs' shell. Additionally, in what regards the encapsulation of poly and prepolymeric species of isocyanate, which brings higher reactivity and viscosity to the O phase of the emulsion system, our work can be compared with refs [9, 10]. Haghayegh et al. [9] reported on MCs with mean diameters ranging from 45 ± 1.88 to 250 ± 18.1 μm using an encapsulated isocyanate solution containing 60% of solvent content, by varying the mixing rate, as well as the surfactant concentration. Ma et al. [10] studied the effect of the isocyanate dilution in the final MCs sizes, obtaining MCs with average diameters varying from 62.61 ± 21.90 μm with 30% of solvent and 473.86 ± 214.83 μm without solvent addition. The MCs reported in the present work were obtained using a low solvent content of 25 wt%, less than half the amount used in [9]. When comparing with [10], it is important to consider that we are reporting on the encapsulation of the oligomeric Ongronat®2500 which has a high viscosity of 520–680 cP at 25 °C in contrast to PAPI, whose viscosity ranges 150–220 cP at 25 °C (PAPI 27). Considering the previous results, it is possible to conclude that the obtained MCs in the present paper have reasonable small sizes, varying from 58 μm for the Ref_MCs to 150 μm for the n-OTES_MCs, when encapsulating a highly reactive isocyanate, with a higher viscosity and a lower solvent content.

Figure 4 shows the normalized FTIR spectra of the reagents, active H sources and isocyanates used in the syntheses, while Fig. 5 shows the normalized FTIR spectra of the obtained MCs.

The success of the isocyanate encapsulation can be confirmed from the presence, in all the MCs' FTIR spectra (Fig. 5), of an intense band peaked at ca. 2260 cm^{-1}, which is related to the presence of a N=C=O bond stretching vibration from unreacted isocyanate. The MCs' shell PU and PUa composition
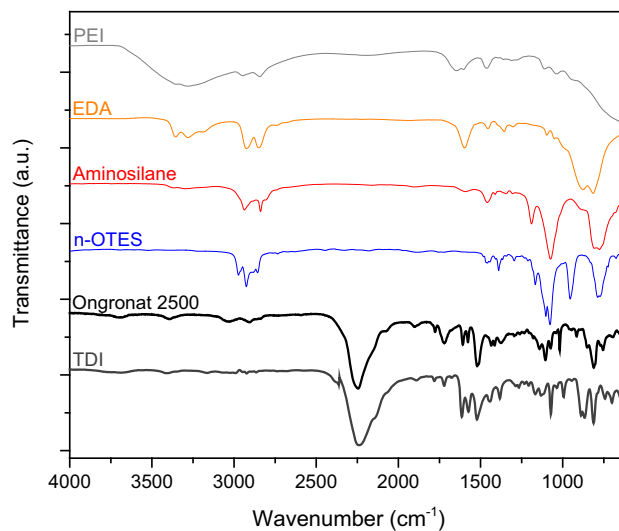
Figure 4 FTIR spectra of the isocyanates and active H sources employed in this work.
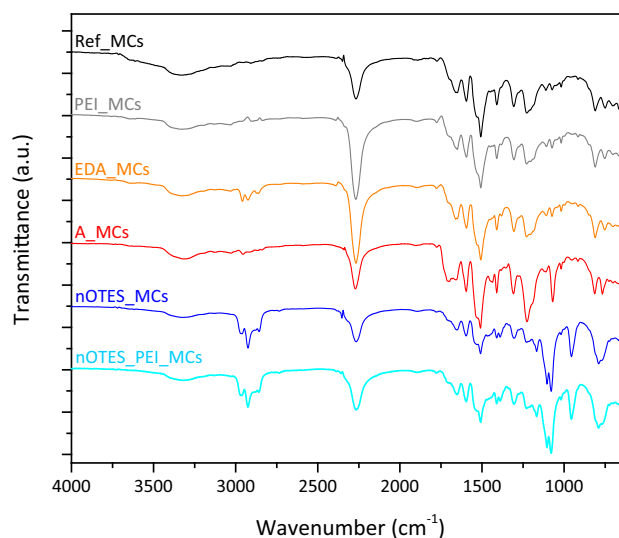
Figure 5 FTIR spectra of the varied MCs obtained.

can be confirmed by the presence of carbonyl groups, either from urethane and urea, detected at 1730–1715 cm^{-1} and at 1700–1680 cm^{-1}, respectively, from the presence of C–O–C group at 1214 cm^{-1} and C–O stretching at 1300 cm^{-1}. Regarding the peaks ascribed to the carbonyl groups, it should be noted that the largest contribution comes from those from urea, for all samples, except A_MCs. This reveals that the hydrolysis of aminosilane when added to the aqueous phase is quite effective, resulting in a large number of silanol (i.e. OH) groups available to react with the NCO of the oil phase, and, therefore, in a majority of urethane bonds within the shell. The

remaining MCs exhibit a shell mainly composed of PUa.

Also, a significant contribution of silane n-OTES structure in the MCs' shell made from this "latent" active H source is visible in the FTIR spectra of nOTES_MCs and nOTES_PEI_MCs, namely in what regards the CH stretching at 3000–2800 cm^{-1} and the region between 1200 and 700 cm^{-1} of the spectrum.

Figure 6 shows a magnification of the MCs and isocyanates' FTIR spectra, for the band ascribed to the N=C=O bond stretching vibration, peaked at ca. 2260 cm^{-1}. A conclusion about the nature of the encapsulated isocyanate compound can be drawn by analysing this peak.

Comparing the FTIR spectra (Fig. 6) from the isocyanates employed in the syntheses (2,4 TDI and Ongronat$^{®}$ 2500) and that from the encapsulated isocyanates in the resulting MCs, it is possible to observe a blue shift of the FTIR peak ascribed to the encapsulated isocyanate NCO species. In fact, the NCO peak from both the isocyanate sources employed in the syntheses displays its maximum at lower wavenumbers (lower vibration energies) and has a larger full width at half maximum than the FTIR peak of the encapsulated isocyanate NCO species.

The composition and monomeric nature of 2,4 TDI compared to Ongronat$^{®}$ 2500 (oligomeric type of MDI) result in a lower force constant of the bonds and in lower energy of the N=C=O bond stretching
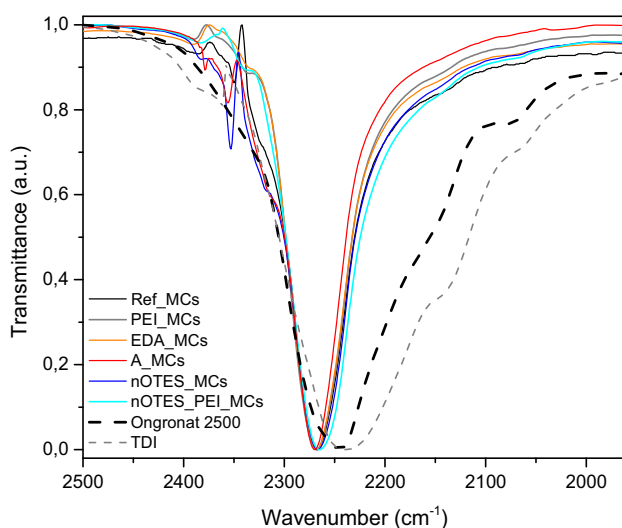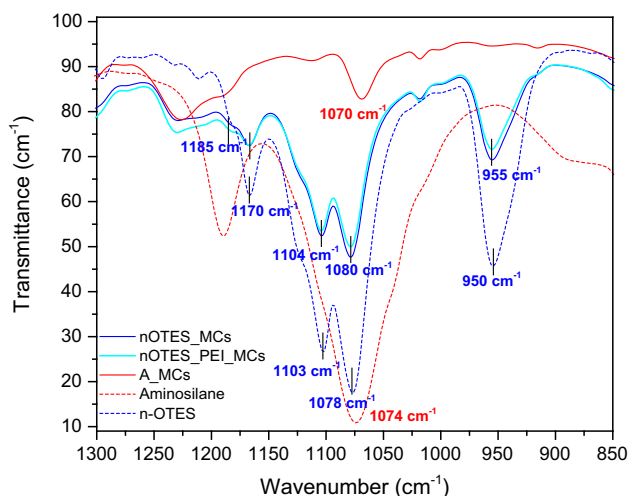

Figure 6 Magnification of the peak assigned to the isocyanate NCO bond stretching, for the obtained MCs and isocyanates used in this study.

vibration. In fact, the movement restrictions within the oligomeric network characteristic of Ongronat$^{®}$ 2500 might require more energy for the bonds to vibrate, leading to the observed shift of the N=C=O peak to higher wavenumbers. Also, the wide NCO peak observed for the monomeric species of 2,4 TDI is consistent to that found in the literature [23]. As it is possible to observe, the NCO peak of all the MCs is located roughly at the same wavenumber, indicating that all the syntheses led to the encapsulation of the same isocyanate (free NCO) species. Also, the location of the NCO peak of the MCs at higher wavenumbers might reveal that Ongronat$^{®}$ 2500 is the NCO compound predominantly encapsulated, while the 2,4 TDI monomers act as shell forming agent. In fact, 2,4 TDI monomers are known to exhibit higher reactivity than MDI oligomers and their lower molecular weight, smaller size and higher polarity, when compared to MDI, allow more mobility of the species towards the O/W interface and higher diffusion rates, which facilitates the shell formation, known to be a diffusion-controlled process. Indeed, according to Verhoeven et al., rigid oligomer molecules, fast reaction kinetics or the use of a cross-linking system do limit the growth of the intermaterial zone and lead to a diffusion-controlled reaction [24].

It should be stressed that the shift to higher wavenumbers and narrowing observed in the NCO peak of the encapsulated compound indicate that are mostly the Ongronat$^{®}$ 2500' higher-order oligomers that were encapsulated, with the remaining, lower molecular weight species, possibly taking part, along with 2,4 TDI, in the polymerization reactions that lead to the MCs' shell formation. These polymerization reactions can also result in a more homogeneous average molecular weight distribution of the encapsulated species and, therefore, in a narrower NCO FTIR peak. In addition, a hypothesis is raised, concerning this shift and narrowing, which is related to the isocyanate-based oligomers' confinement effect, either by the PU/PUa shell, or within the pores of the shell. Despite involving a different chemistry and scale dimension (nanoscale), the work from Shi and Deng [25] might substantiate our hypothesis. Indeed, when trying to finely disperse ionic liquids, through their physical confinement or encapsulation into silica gel matrix prepared by sol-gel processing, they came across with a nano-effect, or restriction effect, produced from the nanopores of the silica gel, which

resulted in an abnormal FTIR and FTRaman spectra, consisting of a peak shift and narrowing effect. However, according to our experience, such effect on the N=C=O peak is only found to occur in the encapsulation of oligomeric and prepolymeric species of isocyanates. As an example, the work by Attaei et al. [3], which concerns the encapsulation of monomeric IPDI, does not report such effect. Supplementary file, S2 shows that the narrowing and shifting effect observed at the NCO FTIR peak is significantly more pronounced when the isocyanate species are encapsulated, comparing with the same effect on the corresponding non-encapsulated species, even when these species are made to react with the moisture of the air during several days. According to our knowledge, this narrowing effect has never been reported to occur for larger than nanoscale environments, nor has been observed regarding the encapsulation of chemicals, such as isocyanates, in nano or microparticles. It is herein shown to occur for the encapsulation of oligomeric, or prepolymeric NCO species, not being observable in the case of monomeric isocyanates [3]. Figure 7 shows the FTIR spectra magnification of the MCs to which silanes where employed during the synthesis as well as of the active H sources aminosilane and n-OTES, in the range between 1300 and 850 cm^{-1}.

From Fig. 7, it is possible to identify the aminosilane' Si-alkoxy groups (Si-O-CH$_3$) by a strong peak at 1075 cm^{-1} and the n-OTES' Si-O-CH$_2$-CH$_3$ group by a peak at 950 cm^{-1} in addition to a strong doublet peaked at 1103 cm^{-1} and 1078 cm^{-1}.

Figure 7 Magnification of the peaks associated with the presence of sílica, Si-alkoxide and siloxane groups.

During the MCs' synthesis, the silanes' alkoxy groups, when added to the water phase, tend to hydrolyze, leading to the formation of silanol groups, with peaks present at ca. 3750 cm^{-1} and ca. 950 cm^{-1} [26]. The silanol groups may react among each other by polycondensation reactions, leading to the formation of siloxane moieties, but also with the isocyanate' NCO groups, when located at the emulsion isocyanate droplet surface, leading to the formation of urethane moieties. It is considered that the silanes act as "latent" active H sources, since they still need to suffer hydrolysis reactions within the aqueous phase of the emulsion, in order to have active H groups to react with NCO, contributing to the MCs' shell formation [3].

It has been reported that the peak related with the Si–O–Si asymmetric stretching vibrations (TO component) is located at ca. 1070 cm^{-1}, whereas the presence of a shoulder at ca. 1200 cm^{-1} corresponds to the LO component of the asymmetric stretch [26]. The presence of a peak at 1074 cm^{-1} and at 1185 cm^{-1} in the A_MCs' spectra might confirm the presence of siloxane moieties in the MCs' shell and, therefore, its hybrid character. Regarding the FTIR spectra of the MCs to which n-OTES was added, there is a strong dominance of the n-OTES fingerprint, which masks any other peak that could reveal the presence of siloxane bonds. So, in this latter case, it was not possible to show an evidence of the hydrolysis and condensation of the silane, neither of the hybrid character of the nOTES_MCs and nOTES_PEI_MCs. This is in line with the fact that the n-OTES-based MCs have an oily appearance.

Also, Fig. 5 exhibits a stronger FTIR peak ascribed to the carbonyl group from urea, than from urethane, contrary to what is observed for A_MCs. This fact also suggests that, if there are Si-OH groups being formed during the synthesis of the n-OTES-based MCs, they are in much less quantity than for A_MCs, leading to less urethane moieties formation.

The following equation, Eq. 1, was used as a relative measure to determine the MCs' isocyanate encapsulation efficiency. For that purpose, the peak at 2260 cm^{-1}, ascribed to the NCO stretching and the peak at 1300 cm^{-1}, assigned to the C-O stretching, related to the PUa/PU shell and which does not significantly change over time, were considered. The peaks area was obtained using the OriginPro2016 software. The equation is as follows:

$$Y = \frac{Area_{NCO(2260 \text{ cm}^{-1})}}{Area_{shell(1300 \text{ cm}^{-1})}} \quad (1)$$

where Y is considered an indirect measure of the isocyanate encapsulation efficiency, $Area_{NCO(2260 \text{ cm}^{-1})}$ the area of the isocyanate' NCO peak and $Area_{shell(1300 \text{ cm}^{-1})}$ the area of the C-O stretching peak, related to the MCs' shell material. In order to study the MCs shelf life, FTIR spectra were taken at four different times: right after the synthesis and 1, 3 and 7 months afterwards, being the MCs exposed, in the meantime, to a temperature of ca. 25 °C in an atmosphere of 50% of relative humidity (RH). The obtained Y values are reported in Table 3, Y is obtained from the FTIR taken after the synthesis, Yi is the direct value calculated using the above equation and the remaining Ys are given as a percentage of Yi. By comparing the Y values obtained over time, it is possible to conclude about the MCs' shell moisture barrier capability. If the MCs' shell does not offer enough protection, moisture might go through the shell, reacting with the free NCO groups in the MCs' core and leading to the loss of the encapsulated compound together with the increase in the shell's thickness, with a consequent decrease in the Y value. As it is possible to observe in Table 3, all the MCs to which active H sources were added during the synthesis present higher encapsulation efficiency, denoted by the higher Y value, than the Ref_MCs. Indeed, the faster formation of the MCs' shell, due to the reaction between the NCO groups from TDI and the extra active H sources, creates an early barrier between the NCO groups and the aqueous medium, leading to a higher amount of encapsulated isocyanate.

The active H source molecules (the amino compounds and silanes) present at the oil droplets surface are known to become in contact and react with the NCO groups from the isocyanate species. Silanol (Si-OH) groups, derived from the silanes, lead to urethane moieties formation, while the NH groups, with a higher reaction rate with isocyanates than OH groups, lead to urea moieties formation. Both contribute to a quicker primary shell formation. For the Ref_MCs, the formation of the shell is only due to the reaction between the isocyanate and the less reactive OH groups from the water, leading to a later formation of the shell and more exposure of the isocyanate with the water phase and, consequently, to a lower encapsulation content [21].

Right after the synthesis, EDA_MCs are the ones that exhibit a higher Y, or encapsulation efficiency, very similar to that exhibited by PEI_MCs, nOTES_MCs and the MCs synthesized using the combination of both PEI and n-OTES. Regarding the A_MCs, the aminosilane only contributes with one NH_2 and a NH group per molecule, and it only has affinity with the oil phase of the emulsion before the hydrolysis reactions take place, which might have affected the emulsion stability at some extent, leading to a poorer encapsulation efficiency. One month after the synthesis, EDA_MCs and PEI_MCs were the ones loosing less isocyanate, only 0.05% of the initial Y value. However, and although all the active H sources contributed to a more protective shell, the best result, corresponding to a loss of only 34% of Yi after 7 months, was obtained for the nOTES_PEI_MCs. Further shelf-life assessment was carried out in this sample, and a loss of only 42% of Yi was achieved for more than 1 year (13 months).

Table 3 MCs' isocyanate relative encapsulation efficiency calculated using the FTIR spectra obtained after the synthesis, 1, 3 and 7 months later. The **Y** obtained after the synthesis is a direct value calculated using (Eq. 1). Y_1, Y_3 and Y_7 are given as a percentage of Yi

Synthesis	Active H source	Yi after the synthesis	Y_1 (%) 1 month after the synthesis	Y_3 (%) 3 months after the synthesis	Y_7 (%) 7 months after the synthesis	Y % lost 7 months after the synthesis
Ref_MCs	–	5.2	37.0	23.2	22.6	77.4
PEI_MCs	PEI	9.8	99.5	51.8	30.8	69.2
EDA_MCs	EDA + Water	9.9	99.5	65.7	51.8	48.2
A_MCs	Aminosilane	6.8	67.7	60.9	56.1	43.9
nOTES_MCs	n-OTES	9.7	63.9	52.4	49.5	50.5
nOTES_PEI_MCs	n-OTES + PEI	7.8	87.5	71.6	66.0	34.0

Indeed, the NH_2 groups present in both EDA and PEI enabled a quicker formation of a PUa shell, leading to a higher encapsulation yield; however, it was the combined effect of PEI and n-OTES, due to n-OTES' hydrophobic side chain, that enabled the most effective barrier against the moisture of the air in a long-term analysis. Part of n-OTES molecules appear to remain non-hydrolyzed and therefore not condensed as observed in Fig. 7; however, their presence in the shell led to the creation of a more effective OH barrier. The aim of the present work was to study the effect of the different active H sources using the same synthesis parameters. However, it should be stressed that better results would be expected, if an optimization of the synthesis conditions was done, with the goal of having a more stabilized emulsion. The stability of the emulsion has been shown to play an important role in the encapsulation process yield and efficiency [27].

Figure 8 shows the thermograms and respective derivative curves of the active H sources as well as of the two isocyanates used in the synthesis, Ongronat® 2500 and 2,4 TDI. As it is possible to observe, the degradation of TDI occurs between 85 and 220 °C, while that of oligomeric MDI, Ongronat® 2500, only occurs at higher temperatures, between 200 and 330 °C, with a later degradation step above 450 °C, which corresponds to higher molecular weight macromolecules. This difference was expected, since TDI is more volatile than MDI (b.p. of 253 °C vs > 300 °C).

Figure 9a shows the thermograms and respective derivative curves of the MCs to which amine-based active H sources were added, while Fig. 9b exhibits the ones corresponding to the MCs with n-OTES in their composition.

It is possible to observe in all the MCs' thermograms a gradual step of weight loss in the range of 200–350 °C, which can be correlated with the decomposition of liquid, unreacted, Ongronat® 2500, in different stages of polymerization (monomers, dimers and trimers), confirming its encapsulation. When comparing with the pure Ongronat® 2500 thermogram, degradation finalizes at slightly higher temperatures, maybe because of the encapsulation effect and/or due to the formation of higher molecular weight species of Ongronat® 2500 during the encapsulation process.

Regarding TDI, it has a lower degradation temperature, between 85 and 220 °C, and is not detected in the Ref_MCs thermogram, indicating that it has indeed reacted to form the PU/PUa MCs' shell. n-OTES_MCs and n-OTES_PEI_MCs show a degradation step between ca. 105–180 °C that can be correlated with the presence of n-OTES in the MCs, due to the degradation of its alkoxy groups as well as the aliphatic hydrocarbon side chain (Fig. 9). The degradation peak present in the aminosilane thermogram, at 190 °C is not present in the A_MCs, confirming that the silanes' alkoxy groups are no longer present in the MCs, confirming that its hydrolysis indeed occurred during the MCs' synthesis. Instead, a peak
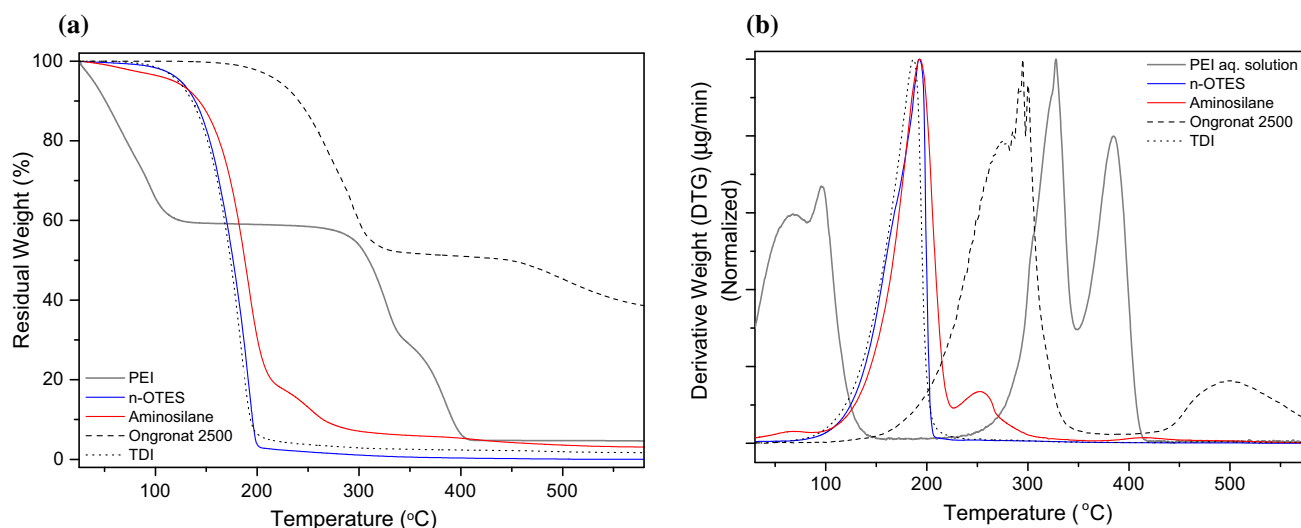
Figure 8 **a** Thermograms of the isocyanates used in the synthesis and the active H sources, PEI (aq. solution at 50 wt%), n-OTES and aminosilane. **b** Respective derivative curves.
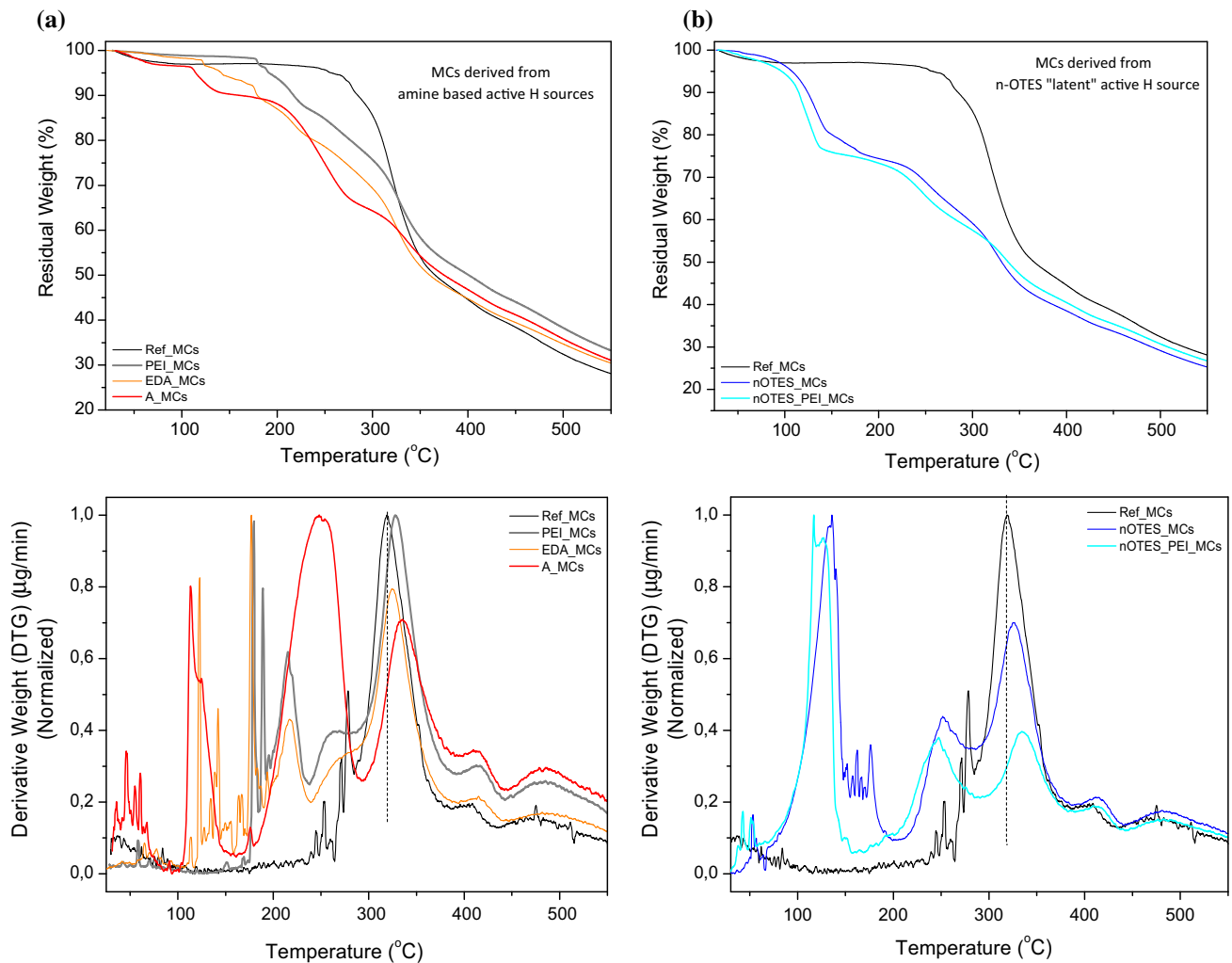
Figure 9 a Thermograms of the MCs to which NH active H sources were added during the synthesis and the Ref_MCs (top) and the respective derivative curves (bottom). **b** Thermograms of the MCs to which n-OTES was added during the synthesis and the Ref_MCs (top) and the respective derivative curves.

at lower degradation temperatures, at around 115 °C, appeared for the A_MCs, which might be correlated with the presence of some silanol groups that might not undergo polycondensation. The A_MCs have an intense decomposition peak at 250 °C, also visible in the aminosilane thermogram, possibly correlated with the silane's side chain, indicating its presence in the MCs' siloxane moieties, overlapping with the degradation of Ongronat® 2500.

The PUa/PU MCs' shell decomposition, especially soft segments, tend to occur typically around 300 °C and above, as observed in Fig. 9, which leads to some overlapping with the Ongronat® 2500 decomposition, making it impossible to accurately determine the real encapsulated isocyanate content trough thermogravimetric analysis. Indeed, it is possible to observe

in the derivative curves, for all the MCs, a weight loss around 320 °C, correlated with the MCs' shell. It is possible to observe, as well, that all the MCs to which active H sources were added, show a shift of the shell degradation peak to higher temperatures, indicating a higher thermal stability of the shell (Fig. 9a, b, bottom). As expected, from the group present in Fig. 9a, bottom, the A_MCs were the ones showing a more thermally stable shell, with a degradation peak appearing 15 °C at higher temperatures than the reference. The siloxane moieties, brought to the shell from the aminosilane, were expected to contribute to an improved mechanical strength and thermal resistance of the MCs, as confirmed. Regarding the MCs' thermogram (derivative curve) present in Fig. 9b, those who showed better performance in terms of

thermal resistance, similar to A_MCs, was the combination of n-OTES and PEI, confirming the success of the combined effect of these two active H sources.

The main application of the MCs developed in this manuscript is for crosslinkers in one component adhesive formulations; however, self-healing coatings might also be a pertinent application for the microencapsulation technology herein reported. It should be stressed that the size of the selected MCs will strongly depend on the primer or topcoat thickness. Their size might be reduced if thin coatings are envisaged. Stirring speed is one potential parameter to play with to achieve smaller MCs when using the chemistries developed in our work. The clear benefit of the MCs reported in this manuscript is their relatively high loading and the type of isocyanate which, besides being a readily available, commercial one, is of high reactivity, in the sense that it quickly establishes a tridimensional network, when compared with the typical isocyanates generally employed for self-healing purposes, such as IPDI or HDI.

Conclusions

This work shows for the first time the microencapsulation of a highly reactive commercially available oligomeric MDI, Ongronat® 2500, which has a large scope of applications, either in the production of rigid PU foams, or as reactive moisture curable healing agent, adhesives hardener, etc. Ongronat® 2500 is encapsulated by a PU/PUa and a PU/PUa–silica hybrid shell, using a one-pot and straightforward approach, which consists of an O/W microemulsion system combined with an in situ polymerization at the interface of the O/W phases. Besides Ongronat® 2500, TDI is also used in small amount to contribute to the shell formation. This process employed just a small amount of organic solvent due to the reduced viscosity inherent to the oil phase. The role played by a variety of amine-based active H sources, namely EDA, aminosilane and branched PEI, and the silane n-OTES that simultaneously acts as a "latent" active H source and a hydrophobic agent is studied in terms of encapsulation efficiency, shelf life, shell's chemical structure and thermal stability. It is possible to conclude that the NH-based active H sources, EDA and PEI, were the ones that led to the achievement of higher encapsulation efficiency, possibly related with

a quicker shell formation. However, the best overall performance was achieved for the combination of the high NH functionality PEI and the silane n-OTES, as active H sources (nOTES_PEI_MCs). These MCs show the best compromise in what regards isocyanate encapsulation efficiency and shelf life. They show a loss of only 34% of the encapsulated compound during a period of 7 months in contrast with the 77.4% lost by the Ref_MCs. Their robustness and effective barrier against air' moisture are critical for their future application as cross-linkers for eco-innovative mono-component adhesive formulations.

Acknowledgements

Compliance with ethical standards

Conflict of interest The authors declare that they have no conflict of interest.

Electronic supplementary material: The online version of this article (https://doi.org/10.1007/s10853-019-04301-1) contains supplementary material, which is available to authorized users.

References

[1] Langenberg KV, Warden P, Adam C, Milner HR (2010) The durability of isocyanate based adhesives under service in Australian conditions, the results from a 3 year exposure study and accelerated testing regime (Literature Review), Melbourne, Australia: Forest & Wood Products Australia Limited; 63 p. https://www.fwpa.com.au/images/processing/PNB034-0506_Literature_Review_Isocyanate_Adhesives_0.pdf. Accessed July 2019

[2] Paiva RMM, Marques EAS, Silva LFM, António CAC, Arán-Ais F (2016) Adhesives in the footwear industry.

Mater. Des. Appl. 230:357–374. https://doi.org/10.1177/1464420715602441

[3] Attaei M, Loureiro MV, Vale M, Condeço JAD, Pinho I, Bordado JC, Marques AC (2018) Isophorone diisocyanate (IPDI) microencapsulation for mono-component adhesives: effect of the active H and NCO sources. Polymers 10:825. https://doi.org/10.3390/polym10080825

[4] Loureiro MV, Vale M, Schrijver AD, Bordado JC, Silva E, Marques AC (2018) Hybrid custom-tailored sol-gel derived microscaffold for biocides immobilization. Microporous Mesoporous Mater 261:252–258. https://doi.org/10.1016/j.micromeso.2017.10.056

[5] Loureiro MV, Lourenço MJ, Schrijver AD, Santos LF, Bordado JC, Marques AC (2017) Effect of operation variables and monomers on the properties of polyamide microcapsules. J Mater Sci 52:5380–5389. https://doi.org/10.1007/s10853-017-0782-6

[6] Loureiro MV, Ciriminna R, Lourenço MJ, Santos LF, Schrijver AD, Bordado JC, Pagliaro M, Marques AC (2017) Organically-modified silica based microspheres for self-curing polyurethane one component foams. Microporous Mesoporous Mater 244:244–250. https://doi.org/10.1016/j.micromeso.2016.10.039

[7] Saunders K (1998) Organic polymer chemistry of adhesives, fibres, paints, plastics, and rubbers, 2nd edn. Chapman and Hall, London

[8] Duan B (2016) in Handbook of encapsulation and controlled release. In: Karsa DR, Stephenson RA (eds) Microencapsulation via in situ polymerization. Woodhead Publishing Limited, Cambridge, pp 307–314

[9] Haghayegh M, Mirabedini SM, Yeganeh H (2016) Microcapsules containing multi-functional reactive isocyanate-terminated polyurethane prepolymer as a healing agent. Part 1: synthesis and optimization of reaction conditions. J Mater Sci 51:3056–3068. https://doi.org/10.1007/s10853-015-9616-6

[10] Ma Y, Jiang Y, Tan H, Zhang Y, Gu J (2017) A rapid and efficient route to preparation of isocyanate microcapsules. Polymers 7:24–27. https://doi.org/10.3390/polym9070274

[11] Yang J, Keller MW, Moore JS, White SR, Sottos NR (2008) Microencapsulation of isocyanates for self-healing polymers. Macromolecules 41:9650–9655. https://doi.org/10.1021/ma801718v

[12] Sondari D, Septevani AA, Randy A, Triwulandari E (2010) Polyurethane microcapsule with glycerol as the polyol component for encapsulated self healing agent. IJET 2:446–471

[13] Di Credico DB, Griffini G, Levi M, Turri S (2013) Microencapsulation of a UV-responsive photochromic dye by means of novel UV-screening polyurea-based shells for smart coating applications. ACS Appl Mater Interfaces 5:6628–6634. https://doi.org/10.1021/am401328f

[14] Kardar P (2015) Preparation of polyurethane microcapsules with different polyols component for encapsulation of isophorone diisocyanate healing agent. Prog Org Coat 89:271–276. https://doi.org/10.1016/j.porgcoat.2015.09.009

[15] Ming Y, Hu J, Xing J, Wu M, Qu J (2016) Preparation of polyurea/melamine formaldehyde double-layered self-healing microcapsules and investigation on core fraction. J Microencapsul 33:307–314. https://doi.org/10.1080/02652048.2016.1178352

[16] Huang M, Yang J (2011) Facile microencapsulation of HDI for self-healing anticorrosion coatings. J Mater Chem 21:11123–11130. https://doi.org/10.1039/C1JM10794A

[17] Wu G, An J, Tang XZ, Xiang Y, Yang J (2014) A versatile approach towards multifunctional robust microcapsules with tunable, restorable, and solvent-proof superhydrophobicity for self-healing and self-cleaning coatings. Adv Func Mater 24:6751–6761. https://doi.org/10.1002/adfm.201401473

[18] Nguyen L-TT, Hillewaere XKD, Teixeira RFA, Berg OVD, Prez FED (2014) Efficient microencapsulation of a liquid isocyanate with in situ shell functionalization. Polym Chem 6:1159–1170. https://doi.org/10.1039/C4PY01448K

[19] Zhang M, Ni P, Yan N (1994) Effect of operation variables and monomers on the properties of polyamide microcapsules. J Microencapsul 12:425–435. https://doi.org/10.3109/02652049509087255

[20] Hu M, Guo J, Yu Y, Cao L, Xu Y (2017) Research advances of microencapsulation and its prospects in the petroleum industry. Materials 10:369. https://doi.org/10.3390/ma10040369

[21] Arnold R, Nelson J, Verbanc J (1957) Recent advances in isocyanate chemistry. Chem Rev 57:47–76. https://doi.org/10.1021/cr50013a002

[22] McFarland B, Pojman JA (2015) Effects of shell crosslinking on polyurea microcapsules containing a free-radical initiator. J Appl Polym Sci 132:32. https://doi.org/10.1002/app.42408

[23] Han H, Li S, Zhu X, Jiang X, Kong XZ (2014) One step preparation of porous polyurea by reaction of toluene diisocyanate with water and its characterization. RSC Adv 4:33520–33529. https://doi.org/10.1039/c4ra06383j

[24] Verhoeven VWA, Padsalgikar AD, Ganzeveld KJ, Janssen LPBM (2006) A kinetic investigation of polyurethane polymerization for reactive extrusion purposes. J Appl Polym Sci 101:370–382. https://doi.org/10.1002/app.23848

[25] Shi F, Deng Y (2005) Abnormal FT-IR and FTRaman spectra of ionic liquids confined in nano-porous silica gel. Spectrochimica ActaPart A Mol Biomol Spectrosc 62:239–244. https://doi.org/10.1016/j.saa.2004.12.031

[26] Almeida RM, Marques AC (2018) Handbook of sol–gel science and technology: processing, characterization and applications. In: Klein L, Aparicio M, Jitianu A (eds) Characterization of sol-gel materials by infrared spectroscopy. Springer, BErlin, pp 1121–1151

[27] Cesari A, Loureiro MV, Vale M, Yslas EI, Dardanelli M, Marques AC (2019) Polycaprolactone microcapsules containing citric acid and naringin for plant growth and sustainable agriculture: physico-chemical properties and release behavior. Sci Total Environ. https://doi.org/10.1016/j.scitotenv.2019.135548